

Ordering at Si(111)/*a*-Si and Si(111)/SiO₂ Interfaces

I. K. Robinson, W. K. Waskiewicz, and R. T. Tung
AT&T Bell Laboratories, Murray Hill, New Jersey 07973

and

J. Bohr
Brookhaven National Laboratory, Upton, New York 11973
(Received 11 August 1986)

X-ray diffraction has been used to measure the intensity profile of the two-dimensional rods of scattering from a single interface buried inside a bulk material. In both Si(111)/*a*-Si and Si(111)/SiO₂ examples there are features in the perpendicular-momentum-transfer dependence which are not expected from an ideal sharp interface. The diffraction profiles are explained by models with partially ordered layers extending into the amorphous region. In the Si(111)/*a*-Si case there is clear evidence of stacking faults which are attributed to residual 7×7 reconstruction.

PACS numbers: 68.35.Bs, 68.55.Jk

Interfaces between crystals and between crystalline and amorphous materials have many properties in common with surfaces, and much could be learned from the application of surface structural-analysis techniques to them. Because so many of such techniques involve non-penetrating probes, this has not been possible in general, and many details of the atomic arrangements of interfaces remain undiscovered. Little is known about interfacial roughness, the stabilization of new periodicities (interfacial reconstruction), and relaxation of perpendicular layer spacings. A very important question relating to the physics of epitaxy is to what extent order propagates from a crystal into an adjacent amorphous material.

The Si(111)/*a*-Si interface which we have chosen to study has been the subject of several recent investigations.¹⁻⁴ From cross-sectional electron microscopy it has been claimed that grains of amorphous silicon (*a*-Si) are orientationally oriented with respect to a crystal substrate nearby.¹ A plan-view transmission-electron diffraction study has shown that the 7×7 periodicity of clean reconstructed Si(111) is preserved at the interface.² This interface must bear some structural resemblance to the clean surface state, and the differences should contain clues about the mechanism of Si growth on Si. Si/SiO₂ interfaces are extremely flat even after growth of thousands of angstroms of oxide: This is known from sectional transmission electron microscopy (TEM)³ as well as low-energy electron diffraction (LEED) after stripping.⁴ There are even unsolved questions about the Si(111)-surface structure, which carry over to Si(111) interfaces. This is especially true of the vertical structure which has been a subject of recent debate.^{5,6}

It is by now well established that traditional x-ray diffraction methods, enhanced by use of synchrotron radiation, can be used to study isolated monolayer structures,

such as liquid-crystal films,⁷ rare gases adsorbed on graphite,⁸ and reconstructed surfaces.⁹ Recently we have shown¹⁰ that even unreconstructed surfaces give rise to the rodlike scattering characteristic of two-dimensional (2D) objects. The so-called crystal truncation rods (CTR) which appear are due to the termination of the crystal lattice at a surface. The CTR profile is related to the abruptness of the crystal-vacuum interface, so that surface roughness information can be obtained.^{10,11} These principles neatly carry over to the study of interfaces with the use of x rays, which is our present subject.

Previously, the observed CTR intensity was always uniformly lower than the ideal curve for a perfectly truncated crystal, and this was attributed to roughness.¹⁰ In this paper we present new diffraction results with an unprecedented *oscillatory modulation* of the rod profiles, and show that this can be attributed to specific structures at the interface: The Si(111)/*a*-Si interface has reversed stacking over half of each of the three layers which are ordered. We interpret this to be a direct consequence of reconstruction in the substrate.^{12,13} Conversely the Si(111)/SiO₂ interface is satisfactorily explained by three fractionally ordered layers and no reversed stacking.

Lightly doped *n*-type Si(111) wafers (~1 Ω cm) were used. They were degreased and cleaned chemically by repeated oxide growth and removal.¹⁴ A final protective oxide was grown¹⁴ and samples were introduced into a molecular-beam epitaxy system (base pressure < 10⁻¹⁰ τ). After outgassing, the samples were cleaned by heating to 800 °C for 1 min to give sharp LEED patterns and uncontaminated Auger-electron spectra. Si(111)/*a*-Si interfaces were then formed by electron-beam deposition of 50–70 Å of Si at room temperature. These were also found to be reconstructed as evidenced by 1/7th-order x-ray diffraction peaks; this confirms the

results of previous electron-diffraction studies.² The Si(111)/SiO₂ sample was made by thermal oxidation until an oxide layer of 1000 Å was obtained. No $\frac{1}{7}$ th-order diffraction was detected.

X-ray diffraction measurements were made on beam-line VII-2 at the Stanford Synchrotron Radiation Laboratory by use of focussed wiggler radiation of 1.3-Å wavelength, a double Si(111) monochromator, and a four-circle diffractometer operating in the symmetric ($\omega=0$) mode.¹⁵ The sample was mounted in a roughing vacuum enclosure with the (111) crystal plane of the interface accurately aligned perpendicular to ϕ axis.¹⁵ No analyzer was used; instead, a 2×10 mm slit was placed in front of the scintillation detector. This gave relatively high background levels and poor 2θ resolution, but was the key to obtaining high accuracy. The symmetric geometry, with equal angles of incidence and exit at the samples, ensured maximum penetration to the interface; by keeping the angle of incidence always larger than 1° , attenuation problems as well as possible refraction artifacts were avoided completely.

A hexagonal (h) unit cell for Si was chosen for all calculations by a coordinate transformation from cubic (c) in reciprocal space:

$$\begin{aligned} (100)_h &= \frac{1}{3}(4\bar{2}2)_c, & (010)_h &= \frac{1}{3}(2\bar{2}4)_c, \\ (001)_h &= \frac{1}{3}(111)_c. \end{aligned} \quad (1)$$

Thus momentum transfer in the direction normal to the interface is represented by a pure index l . Figure 1 shows measurements of the $(10l)_h$ and $(01l)_h$ rods, continuous functions of l which pass through bulk Bragg reflections at $(105)_h = (311)_c$, $(011)_h = (11\bar{1})_c$, $(014)_h = (220)_c$, and $(017)_h = (331)_c$. Since measurements were only permitted for $l > 0$, because the interface could not be reached from behind the sample, the two rods are combined as a single plot by means of the bulk-symmetry transformation $(10l)_h \equiv (01l)_h$. Each of the

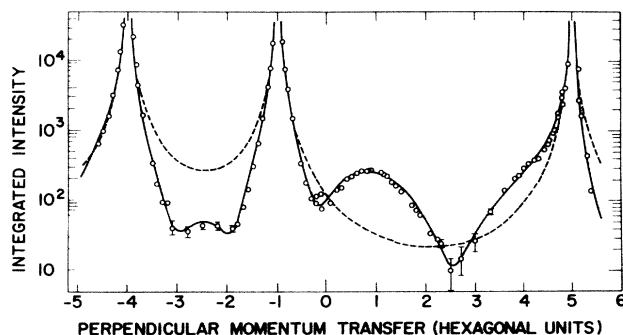


FIG. 1. Measurement of the integrated intensity of the $(10l)_h$ and $(01l)_h$ crystal truncation rods for the Si(111)/*a*-Si interface as a function of l . The two profiles have been merged at $l=0$. The intensity diverges at three bulk Bragg reflections; reliable subtraction of thermal diffuse scattering was not possible closer than shown.

92 measured points corresponds to a rocking scan of the diffractometer θ angle showing a resolution-limited peak at the position of the CTR. The intensity was integrated and background subtracted, then corrected for Lorentz factor $(\sin 2\theta)^{16}$ and changes in active area $(\sin 2\theta)^{17}$. Finally the Si form factor was divided out¹⁶ to obtain the square of the structure factor.

The exact functional form for the CTR structure factor¹⁰ of a diamond lattice ending with a $(111)_c$ "double layer" can be shown to be

$$|F(10l)_h| = \frac{\cos[\pi(4+l)/12]}{\sin(\pi l)} \{1 + 2\cos[2\pi(1+l)/3]\}. \quad (2)$$

This has the l^{-1} divergence at the Bragg peaks $l=5, -1, -4, -7$, but not at $l=2$ which is systematically absent in diamond [$(102)_h = (200)_c$]. The square of Eq. (2) is plotted as the dashed curve in Fig. 1, which fits a scale factor and Debye-Waller factor to the measurements closest to the Bragg peaks.

While the data do bear some resemblance to this ideal curve, an additional modulation is present which must be attributed to the details of the interfacial structure. The data show broad maxima near $l=1$ and $l=4$ where the measured intensity actually exceeds the theoretical value for an ideal truncated surface. Because these mimic the Bragg peaks at $l=-1$ and $l=-4$, we are persuaded that some layers with reversed stacking sequence, whose diffraction pattern is the mirror image in the $(111)_c$ plane, are present at the interface.

The solid curve in Fig. 1 was obtained by building the model of Fig. 2 and least-squares refining its parameters. We assume bulk crystal from $z = -\infty$ to $z = 0$ with normal diamond stacking, $\cdots AaCcBbAa |$, where the letter

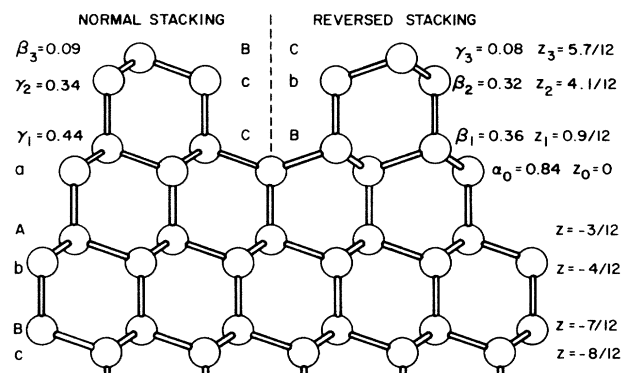


FIG. 2. Model of the Si(111)/*a*-Si interface and refined parameter values. Regions with normal stacking sequence $\cdots cBbAaCcB$ and reversed sequence $\cdots cBbAaBbC$ coexist in the interface. Parameters a_j , β_j , and γ_j are statistical occupancies (in units of monolayers) of sites A, B, and C in the j th layer above the interface. Parameters z_j are layer heights in fractions of the hexagonal unit cell parameter ($\sqrt{3}a_0 = 9.41$ Å).

denotes the registry and upper case refers to the upper half of a double layer. The "a" layer at $z_0=0$ is allowed to have partial occupancy, α_0 . The next layer at $z_1 = \frac{1}{12}$ (hexagonal crystallographic units) has fraction β_1 of "B" (reversed stacking) and fraction γ_1 of "C" (normal). On top of this comes a layer at $z_2 = \frac{4}{12}$ with fraction β_2 of "b" and γ_2 "c." Three extra layers altogether were needed to obtain a good fit. After the layer occupancies had refined, the heights z_1 to z_3 were also allowed to vary. Parameter uncertainties were around ± 0.05 monolayers in occupancy and $\pm 0.1/12$ (0.08) Å in position.

Our analysis up to this point has provided a model to explain the diffraction data. We have made no assumptions about the origins of its components, yet when we compare it with the accepted model of clean reconstructed Si(111)7×7,^{12,13} there is a very obvious correspondence. From the Takayanagi model¹² the layer containing dimers appears here at $z=0$; the layer with "stacking faults" at $z_1 = \frac{1}{12}$; the layer with adatoms has vanished altogether. The theoretical layer occupancies from that model assuming a dimer displacement of $\Delta=0.17$ unit cells¹³ would be $\alpha_0 = [40 + 8 \cos(2\pi\Delta)]/49 = 0.89$, $\beta_1 = \gamma_1 = \frac{21}{49} = 0.43$. All three coefficients are close to our determined values. The layers at $z_2 = \frac{4}{12}$ and $z_3 = \frac{5}{12}$ are not in the Takayanagi structure and must therefore be ordered layers originating from the *a*-Si. The first extra layer (z_2) is 80% ordered relative to the layer beneath; this is reasonable because these bonds are perpendicular to the interface. The second extra layer (z_3) is only 25% ordered relative to z_2 . Layerwise ordering on the amorphous side of the Si(111)/*a*-Si interface was also seen by sectional TEM,² although the exact location of the interface was unclear; here the interface is unambiguously located by the presence of reversed stacking. Finally, we note that the slight asymmetry between the normal and reversed stacking regions can be explained by occasional variations of the interface height over the 5000-Å coherence length.

The average layer spacings in the newly ordered region are somewhat expanded from the ideal values for the diamond lattice. The most significant of these, $z_3 - z_2 = \frac{1}{12}$ is probably due to the disorder in the top layer: An atom in z_3 with only one or two bonds to the z_2 layer will tend to be higher up if the bonds can bend slightly. The layer spacings in the reconstructed region show no significant departure from ideality. When the position z_0 was allowed to vary, no significant change was found either. We conclude that the bonding in the reconstructed interface is relatively unstrained, in contrast to x-ray standing-wave studies of the clean reconstructed surface,⁵ which see a contraction of $\frac{0.6}{12}$ of a hexagonal unit cell (0.5 Å), but in agreement with standing-wave measurements of a Ge monolayer buried at the Si(111)/*a*-Si interface.⁶

Figure 3 shows analogous measurements of the (101)_h

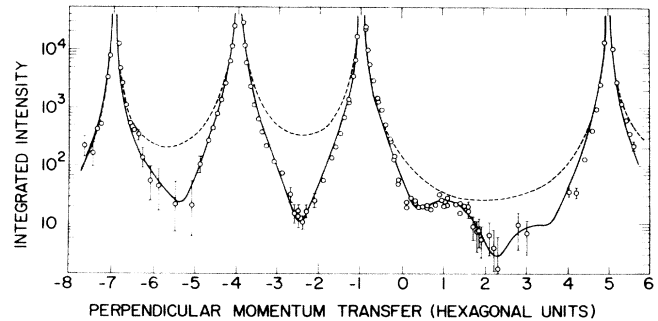


FIG. 3. Measurement of the Si(111)/SiO₂ interface, as in Fig. 1.

and (011)_h rods for the Si(111)/SiO₂ interface. The same model of Fig. 2 was used to obtain the fit, but with the reversed occupancies $\beta_1 = \beta_2 = \gamma_3 = 0$. The refined values of the remaining layer occupancies were $\alpha_0 = 1.03$, $\gamma_1 = 0.75$, $\gamma_2 = 0.32$, $\beta_3 = 0.26$, and the layer positions $z_1 = 0.9$, $z_2 = 4.1$, $z_3 = 5.0$. These values assume that the ordered atoms are Si: We cannot tell whether any ordered O is present. Our interpretation of this result is that the Si(111)/SiO₂ interface is extremely flat, with the partial occupancy of the upper double layer (z_2 and z_3) being due to monolayer height variations over the 5000-Å instrumental coherence length. This agrees with electron-microscope observations.³

We may now consider the implications of our results for the mode of interface growth. When *a*-Si is deposited on the clean reconstructed Si(111)7×7 surface at room temperature, enough energy is released apparently for the bonds connecting the adatoms to be broken, but not enough for the "stacking fault" and dimer features of the structure to be disturbed. The "dangling bond" contribution to the free energy of a surface in vacuum disappears when an *a*-Si interface forms; the adatoms, which each saturate three would-be dangling bonds in the "stacking fault" layer, become destabilized. The first *a*-Si layer attaches with high efficiency to the "stacking fault" instead, and occupies the "atop" site (see Fig. 2). The next layer in the amorphous region is only partially ordered, with a configuration that is far from ideal, as evidenced by the enlarged layer spacing. It is significant that the "stacking fault" and dimer configuration is *not* altered: Presumably at elevated temperatures it becomes unstable and the topological rearrangement necessary to form bulk Si takes place. Such is the nature of epitaxial growth.

X-ray rod profile analysis is likely to become a very general technique for investigating interface structures. The use of x rays allows access to buried interfaces that less-penetrating probes cannot reach. Diffraction from the bulk substrate appears only at singular points which are excluded from the analysis, while the contributions from the unordered amorphous region are diffuse in all directions (except the specular line) and so are subtract-

ed as background. Thus we separate for analysis only the diffraction that is localized in 2D, but diffuse in the direction normal to the interface. This spatial filtering allows us to pick out a few atomic layers which are ordered at the interface from the $\sim 10^6$ layers of material probed. We note that this technique is analogous to understanding I - V curves in LEED, except, of course, the kinematical approximation accurately holds in the x-ray case. It was the observation of mirror images of Bragg peaks in integer-order LEED data, just as in Fig. 1, that led to the original proposal that "stacking faults" were involved with the Si(111)7 \times 7 surface.¹⁸

We would like to thank the Stanford Synchrotron Radiation Laboratory and its staff for their hospitality and L. C. Feldman and J. D. Axe for helpful discussions. The Stanford Synchrotron Radiation Laboratory is supported by the U. S. Department of Energy (Office of Basic Energy Sciences) and the National Institutes of Health Biotechnology Resource Program. Work performed at Brookhaven National Laboratory was supported by the U. S. Department of Energy (Division of Materials Research) under Contract No. DE-AC02-76-CH00016.

¹A. Ourmazd, J. C. Bean, and J. C. Phillips, Phys. Rev. Lett. **55**, 1599 (1985).

²J. M. Gibson, H. J. Gossmann, J. C. Bean, R. T. Tung, and L. C. Feldman, Phys. Rev. Lett. **56**, 355 (1986).

³O. L. Krivanek, D. C. Tsui, T. T. Sheng, and A. Kamgar, in *Physics of SiO₂ and its Interfaces*, edited by S. T. Pantelides

(Pergamon, New York, 1978), p. 356.

⁴P. O. Hahn and M. Henzler, J. Appl. Phys. **52**, 4122 (1981).

⁵S. M. Durbin, L. E. Berman, B. W. Batterman, and J. M. Blakely, Phys. Rev. Lett. **56**, 236 (1986).

⁶J. R. Patel, J. A. Golovchenko, J. C. Bean, and R. J. Morris, Phys. Rev. B **31**, 6884 (1985).

⁷D. E. Moncton and R. Pindak, Phys. Rev. Lett. **43**, 701 (1979).

⁸K. L. D'Amico, D. E. Moncton, E. D. Specht, R. J. Birgeneau, S. E. Nagler, and P. M. Horn, Phys. Rev. Lett. **53**, 2250 (1984).

⁹P. M. Eisenberger and W. C. Marra, Phys. Rev. Lett. **46**, 1081 (1981); I. K. Robinson, Phys. Rev. Lett. **50**, 1154 (1983); J. Bohr, R. Feidenhans'l, M. Nielsen, M. Toney, R. L. Johnson, and I. K. Robinson, Phys. Rev. Lett. **54**, 1275 (1985).

¹⁰I. K. Robinson, Phys. Rev. B **33**, 3830 (1986).

¹¹S. R. Andrews and R. A. Cowley, J. Phys. C **18**, 6427 (1985).

¹²K. Takayanagi, Y. Tanishiro, S. Takahashi, and M. Takahashi, Surf. Sci. **164**, 367 (1985).

¹³I. K. Robinson, W. K. Waskiewicz, P. H. Fuoss, J. B. Stark, and P. A. Bennett, Phys. Rev. B **33**, 7013 (1986).

¹⁴A. Ishizaka and Y. Shiraki, J. Electrochem. Soc. **133**, 666 (1986).

¹⁵W. R. Busing and H. A. Levy, Acta Crystallogr. **22**, 457 (1967).

¹⁶B. E. Warren, *X-Ray Diffraction* (Addison-Wesley, Reading, MA, 1969).

¹⁷I. K. Robinson, in *Surface Crystallography*, Handbook on Synchrotron Radiation Vol. 3, edited by D. E. Moncton and G. S. Brown (Springer-Verlag, New York, 1986).

¹⁸P. A. Bennett, L. C. Feldman, Y. Kuk, E. G. McRae, and J. E. Rowe, Phys. Rev. B **28**, 3656 (1983).